Mesoscale Assimilation of TMI Rainfall Data with 4DVAR: Sensitivity Studies

Zhaoxia Pu
Goddard Earth Sciences and Technology Center
University of Maryland, Baltimore County
NASA Goddard Space Flight Center

Wei-Kuo Tao
Laboratory for Atmosphere
NASA Goddard Space Flight Center

To be submitted to *Journal of Meteorological Society of Japan*

Popular Summary

TRMM (Tropical Rainfall Measurement Mission) offers a unique opportunity to improve the understanding of tropical meteorology and to evaluate the impact of rainfall data on tropical weather forecasts. Early studies demonstrated that assimilation of the TRMM microwave imager (TMI) derived rainfall data into *large-scale global model* is beneficial for the analysis of atmospheric general circulation (Hou et al. 2000) and also consequently can have significant impact on mesoscale forecast of Supertyphoon Paka (1997) (Pu et al. 2002). Instead of direct assimilation of rainfall data into the global model as in Hou et al. (2000), this paper evaluates the impact of TMI rainfall on mesoscale forecast via the *direct assimilation of* the TMI-derived rainfall rate *into the mesoscale regional model* itself using a four-dimensional variational data assimilation (4DVAR) technique.

Sensitivity studies are performed on the assimilation of TMI-derived rainfall data into a mesoscale model using a four-dimensional variational data assimilation (4DVAR) technique. A series of numerical experiments is conducted to evaluate the impact of TMI rainfall data on the numerical simulation of Hurricane Bonnie (1998). The results indicate that rainfall data assimilation is sensitive to the error characteristics of the data and the inclusion of physics in the adjoint and forward models. In addition, assimilating the rainfall data alone is helpful for producing a more realistic eye and rain bands in the hurricane but does not ensure improvements in hurricane intensity forecasts. Further study indicated that it is necessary to incorporate TMI rainfall data together with other types of data such as wind data into the model, in which case the inclusion of the rainfall data further improves the intensity forecast of the hurricane. This implies that proper constraints may be needed for rainfall assimilation.

In addition, as the coverage of TMI data is very limited for the regional applications, the use of merged multi-satellite data or future Global Precipitation Mission (GPM) data products will be necessary for future applications.

Mesoscale Assimilation of TMI Rainfall Data with 4DVAR: Sensitivity Studies

Zhaoxia Pu *

Goddard Earth Sciences and Technology Center

University of Maryland, Baltimore County

NASA Goddard Space Flight Center

Wei-Kuo Tao

Laboratory for Atmosphere

NASA Goddard Space Flight Center

Submitted to *Journal of Meteorological Society of Japan*

September 25, 2003

Corresponding Author: Dr. Zhaoxia Pu, Mail Stop 912, NASA Goddard Space Flight Center, Greenbelt, MD 20771, USA

Email: pu@agnes.gsfc.nasa.gov

ABSTRACT

Sensitivity studies are performed on the assimilation of TRMM (Tropical Rainfall Measurement Mission) Microwave Imager (TMI) derived rainfall data into a mesoscale model using a four-dimensional variational data assimilation (4DVAR) technique. A series of numerical experiments is conducted to evaluate the impact of TMI rainfall data on the numerical simulation of Hurricane Bonnie (1998). The results indicate that rainfall data assimilation is sensitive to the error characteristics of the data and the inclusion of physics in the adjoint and forward models. In addition, assimilating the rainfall data alone is helpful for producing a more realistic eye and rain bands in the hurricane but does not ensure improvements in hurricane intensity forecasts. Further study indicated that it is necessary to incorporate TMI rainfall data together with other types of data such as wind data into the model, in which case the inclusion of the rainfall data further improves the intensity forecast of the hurricane. This implies that proper constraints may be needed for rainfall assimilation.

1. Introduction

The Tropical Rainfall Measuring Mission (TRMM) is a joint Japan-U.S. project to measure rainfall over the global tropics. With the world's first precipitation radar, the TRMM satellite has provided the first detailed and comprehensive dataset on the four-dimensional distribution of rainfall and latent heating over the tropics (between 35° N and 35° S). TRMM offers a unique opportunity to improve the understanding of tropical meteorology and to evaluate the impact of rainfall data on tropical weather forecasts. Early studies have demonstrated that assimilation of TRMM microwave imager (TMI) derived rainfall data into large-scale global models is beneficial for the analysis of the atmospheric general circulation (Hou et al. 2000) and also consequently can have significant impact on mesoscale forecasts [e.g. Supertyphoon Paka in1997 (Pu et al. 2002]. Instead of direct assimilation of rainfall data into the global model as in Hou et al. (2000) and Pu et al. (2002), this paper evaluates the impact of TMI rainfall on mesoscale forecasts via the *direct assimilation* of TMI-derived rainfall rates *into the mesoscale regional model* itself using a four-dimensional variational data assimilation (4DVAR) technique.

The description of the model, the 4DVAR system, the hurricane case, and the TMI data is addressed in section 2 and 3, respectively. Detailed numerical results, including sensitivity studies and forecast impacts, are given in section 4. A summary and discussion are given in section 5.

2. Description of the mesoscale model and 4DVAR system

The Penn State University/National Center for Atmospheric Research (PSU/NCAR) mesoscale forecast model (MM5) and its adjoint system are used in this study. The MM5 is a limited-area, non-hydrostatic primitive equation model with multiple options for various physical parameterization schemes (Dudhia 1993; Grell et al. 1995). The model employs a terrain-following σ vertical coordinate, where σ is defined as $\sigma = (p - p_{top})/(p_{sfc} - p_{top})$, p is pressure, and p_{sfc} and p_{top} are the pressures at the surface and model top, respectively. Physics options used for the forecast model in this study include the Grell cumulus parameterization, a simple ice microphysics scheme (Dudhia 1993), the Blackadar high-resolution planetary boundary layer parameterization scheme (Blackadar, 1976, 1979; Zhang and Anthes 1982), and a cloud atmospheric radiation scheme (Dudhia 1993). The land surface temperature is predicted using surface energy budget equations as described in Grell et al. (1995). For a more detailed description of MM5, see Dudhia (1993) and Grell et al. (1995).

The MM5 adjoint modeling system (Zou et al. 1998) is employed in the data assimilation experiments. For the variational data assimilation system, the physics options in the adjoint model are the Grell cumulus parameterization, a simple ice microphysics scheme (Dudhia 1989), and the Blackadar high-resolution planetary boundary layer parameterization scheme. Application of the MM5 adjoint model to a variety of mesoscale weather systems has been demonstrated in papers by Kuo et al. (1996) and Zou and Kuo (1996).

In general, a 4DVAR system tries to minimize the following cost function:

$$J(x_o) = \sum_{k=1,m} J_k + J_b \ , \qquad (1)$$

where x is the analysis variable and the subscript "0" denotes the initial state. J_b is the background term, and J_k is the contribution to the cost function from an individual type of data. The subscript k denotes the type of data and m is the total number of available data types. For example, the contributions from one arbitrary type of observation can be described as follows:

$$J_k(x_0) = \sum_{i=0,\Delta} \left(H_i(M_i(x_0)) - o_i\right)^T W \left(H_i(M_i(x_0)) - o_i\right) , \tag{2}$$

where O is the observation data, "i" denotes the "*ith*" time step for integration of the non-linear forecast model M, at which the observations are available, and i $\in (0, \Delta)$, while Δ is the length of the assimilation window. W is a weighting factor that depends on the statistical error characteristics of the observational data. H is a so-called observation operator (possibly no-linear), which transfers the grid-space model variable x to the observational type. In order to minimize the cost function, the adjoint of the tangent linear model of the nonlinear forecast model is required (Talagrand 1987).

The effectiveness of the 4DVAR technique for assimilation of precipitation observations has been addressed by Zou and Kuo (1996) and Zupanski and Messinger (1995). However, this paper will further investigate strategies on the assimilation of TMI data particularly.

3. Hurricane Case and TMI rainfall data

The TRMM Microwave Imager (TMI) is one of several TRMM satellite sensors. The TMI measures the horizontal distribution of rainfall by receiving microwaves emitted or scattered by raindrops and ice particles in five microwave channels. At NASA

Goddard Space Flight Center, the TMI microwave radiances are used to retrieve surface rainfall rate information via the Goddard Profiling (GPROF) algorithm. The basis for the rainfall retrieval algorithm is the Bayesian technique described in Kummerow et al. (1996) and Olson et al. (1996, 1999). In order to evaluate the impact of TMI rainfall data on mesoscale forecasts, these retrieved surface rainfall data are assimilated into the MM5 model.

The TMI footprints usually cover the global tropics (35° N-35° S) in a 24-hour period. However, during a typical mesoscale analysis period (usually a 3 h or 6 h period) and for a specific regional domain, there are only limited TMI observations available. In most cases, the TMI samples only about twice a day for a certain region, and the time interval between the swathes may exceed 6 h. Considering the data availability during a 6h analysis cycle, Hurricane Bonnie (1998) was selected from several storm cases to perform the sensitivity studies in this paper.

There were two TRMM swathes that passed over Bonnie in the Atlantic Ocean with a time interval of about 6 h. The two overpasses were around 1139 UTC 22 August 1998 and 1807 UTC 22 August 1998 (Fig.1), respectively. At the time, Bonnie was a category 1 hurricane based on the Saffir-Simpson intensity scale, having recently developed from a tropical storm. 1200 UTC 22 August 1998 was selected as the initial time for the experiments. A 6 h data assimilation window was set for the period 1200 UTC – 1800 UTC August 1998.

Based on TMI-derived surface rainfall data being typically defined as an hourly "rain rate" and the actual data availability, the TMI-derived rainfall was treated as "hourly

(3)

averaged rainfall". Therefore, Eq.(2) can be written as follows:

$$J_k(x_0) = \sum_{i=0,\Delta}\left(\frac{1}{T}\sum_{j=0}^{Tj} CR_{ij} - RR_i\right)^T W_{RR}\left(\frac{1}{T}\sum_{j=0}^{Tj} CR_{ij} - RR_i\right)$$

where T is the averaging time period (i.e., one hour), RR the retrieved TMI rain rate, and CR the model-generated rainfall in the time step.

4. Numerical Experiments and Results

The data assimilation experiments were conducted at 36 km resolution. The model domain is show in Fig.1.

4.1 Sensitivity studies

Numerical experiments were conducted to test strategies for assimilating TMI-retrieved rainfall rates. Two groups of sensitivity studies were performed to test the sensitivity of specification of the error characteristics and the inclusion of physics in the adjoint model to the TMI rainfall data assimilation. Table 1 lists the experimental configuration for all numerical experiments in this paper.

a. Sensitivity of the specified rainfall data error characteristics

The W factor in Eq.2 is a weighting factor that depends on the statistical error characteristics of the observations. To some extent, this factor represents how much the 4DVAR system would "trust" the observations. Because the correlations between the observations are usually unknown or difficult to define, the W matrix is often defined as a diagonal matrix. Three experiments were conducted with the specification of the error characteristics as follows: in Experiment 1, W was set up as a unified number and defined as the inversion of variances based on all available data (i.e., unified W); in

Experiment 2, a 20% error was assumed for the retrieved rainfall rate, and W was defined as the inversion of the error variances (i.e., 20% error); and in Experiment 3, the error characteristics were specified following Bauer et al. (2002) and Olson (personal communication) as:

over ocean $\sigma_s = 1.357\ R^{0.7}$

over land $\sigma_s = 2.516\ R^{0.558}$

where R is the retrieved rain rate and σ_s the standard deviation of the rain rate. The σ_s was obtained from a large sample of retrieved rainfall rate datasets.

Fig.2 shows the variation of the cost-function with the number of iterations. The definition of W mainly impacts the convergence of the minimization in terms of both cost-function reduction and speed of convergence. As a consequence, W effects how much information can be gained from the observations. The results show that it is obviously advantageous to use the error specification suggested by Bauer et al. (2002) and Olson (personal comm.).

b. *Inclusion of physics in the adjoint*

For a common forecast model (forward model), the cumulus parameterization and microphysical processes usually help the model to produce a better rainfall forecast. However, due to the difficulties in deriving an adjoint model for the physics package, in some previous studies (e.g., Zou and Kuo 1996), not all of the physics processes were included in the adjoint model. In order to test the impact of including physics in both the forward and adjoint models on data assimilation results, the following three experiments were conducted: in Experiment 4, both forward and adjoint models include cumulus parameterization but not microphysics; in Experiment 5, both cumulus parameterization and microphysical processes are included in the forward and adjoint models; and in Experiment 6, neither cumulus parameterization nor microphysical process are included in adjoint and forward models. For all Experiment 4~6, the specified error characteristics followed those in Experiment 3.

Fig.3 shows the variation of the cost-function with the number of iterations. As expected, including all of the physics packages has the largest benefit in terms of both convergence and assimilation results.

4.2. Impact on forecasts

Figure 4 shows rainfall rates at the end of the data assimilation (6-h forecast) from Experiment 2 compared with the control experiment (CTRL) where rainfall data were not assimilated. Obviously, assimilating the rainfall data helps the model to produce a more realistic eye and rain bands in the hurricane. The results are quite encouraging. Twenty-four hour forecasts were conducted to test the impact of the rainfall data on the hurricane intensity forecast. Unfortunately, there was no improvement in the consequent forecasts. The forecasted track and intensity (in terms of maximum surface wind and minimum sea level pressure) are almost the same in cases both with and without the TMI rainfall data assimilation (figure not shown), indicating the impact of rainfall data on consequent forecasts is almost negligible. This is not consistent with previous results (Pu et al. 2002).

In order to explore additional strategies for rainfall data assimilation, an additional experiment was performed to assimilate rainfall data along with other data sets. As other conventional data is unavailable for this case, bogus vortex wind information is introduced into the assimilation process. Following Pu and Braun (2001), the bogus wind data was derived from the gradient balance equations as follows:

$$V_g^{bogus}(r) = \left[AB(p_n - p_c)\exp(-A/r^B)/\rho r^B\right]^{1/2} \quad (4)$$

where V_g^{bogus} is the gradient surface wind at radius r, ρ the air density (assumed constant at 1.15 g m^{-3}), p_c the central pressure and p_n the ambient pressure (theoretically at infinite radius, however, here taken from representative values in the hurricane environment). The scaling parameters A and B are defined by maximum wind information. By setting $dV_g/dr = 0$, the radius of maximum surface wind (RMW) is $R_m = A^{1/B}$, and substitution back into (4) gives the maximum wind speed, $V_m = C(p_n - p_c)^{1/2}$, where $C = (B/\rho e)^{1/2}$ and e is the base of the natural logarithm.

Based upon the best available estimates (according to the report from the Hurricane Research Division/AOML/NOAA), the parameters defining the bogus vortex are given by p_c=980hPa centered at (22.3°N, 69.8°W), p_n=1012hPa, V_m=38.6 m s^{-1}, and R_m=120 km. The bogus wind information extends out to a radius of 350km. The surface wind is then extended into the vertical with a vertical profile following Pu and Braun (2001). For the experiments, the specified wind information is assimilated every 10 minutes within the first 30 minutes.

Two sets of numerical experiments were performed in a 6-h assimilation window. In the first experiment (Experiment 7), only bogus wind information was assimilated into the model. In the second experiment (Experiment 8), the rainfall data are incorporated along with the bogus wind information.

Figures 5 and 6 show the rainfall rates at the end of the data assimilation (e.g., 6-h forecasts) for Experiment 7 and 8, respectively. Compared with the TMI observations

(Fig.1b), the rainfall patterns in Fig. 8 are closer to the observed rainfall structure, indicating that assimilation of rainfall data further improves the asymmetric hurricane rainfall structure.

Further comparison is illustrated by histograms of the probability density function (PDF) of 1-h rainfall amounts at the end of the data assimilation (Fig.7). The figure shows that rainfall is generally underestimated in the case with rainfall data assimilation but overestimated in the case without rainfall data assimilation. However, the spectral distribution of rainfall rates is relatively narrow, with only one peak in the case with rainfall data assimilation. When the rainfall data are assimilated into the model, the spectrum of rainfall rates becomes broad with multiple peaks; the heavy rainfall rates (~10mm/hr) are also better represented compared to the case without rainfall assimilation.

Figure 8 shows the time variation of the forecast hurricane intensity in terms of the maximum surface wind and minimum sea-level pressure for the subsequent 24 h forecasts. It indicates that rainfall data assimilation is not only helpful for producing better vortex rainbands but also improves subsequent forecasts. The positive impact shown in this group of experiments indicates that it may be necessary to incorporate TRMM rainfall data together with other types of data such as wind data in order to further improve the intensity forecasts for hurricanes. This implies that some constraints may be needed for rainfall assimilation.

5. Summary and discussion

The main conclusions from numerical experiments with TMI rainfall assimilation in this study are:

- Rainfall data assimilation is sensitive to the error characteristics of the data and the inclusion of physics in the forward and adjoint models, suggesting that it is necessary to use the full physics model in rainfall data assimilation and to take into account the error characteristic of the data;
- Assimilating the rainfall data alone produces a more realistic eye and rain bands in the hurricane but does not ensure improvements in hurricane intensity forecasts. Numerical results indicate that it is necessary to incorporate TRMM rainfall data together with other types of data such as wind data into the model, in which case the inclusion of the rainfall data will further improve the intensity forecast of the hurricane. This implies that some constraints may be needed for rainfall assimilation.

In addition to the TMI data, a similar experiment was performed assimilating surface rainfall data derived (from the same algorithm, i.e. GPROF) from TRMM precipitation radar (PR) for Hurricane Bonnie for the same assimilation window. Fortunately, the PR swathes overlap the TMI swathes in both time and space except that the PR swathes are much narrower than the TMI swathes (i.e., they cover the one third of the TMI swathes, figure not shown). A data assimilation experiment similar to Experiment 3 was performed with the PR data. The results are very similar to those from the TMI data assimilation, suggesting that the PR can also provide useful data sets for rainfall assimilation.

Future studies will be conducted to further confirm the above conclusions, and to explore the possibility of incorporating TMI and PR rainfall with other conventional and satellite data to improve mesoscale precipitation and storm forecasting. On the other hand, the coverage of both TMI and PR data is very limited for regional applications. Therefore, the use of merged multi-satellite data (e.g., Huffman et al. 2001; Huffman and Bolvin 2003) will be another alternative option for future study. However, since the Global Precipitation Mission (GPM) is under preparation, a large benefit to NWP could be obtained from that global precipitation data.

Acknowledgements

This work is supported by the NASA Headquarters Atmospheric Dynamics and Thermodynamics Program, and by the NASA TRMM/GPM project. The authors are grateful to Dr. R. Kakar (NASA/HQ) for his support of this research. We thank Dr. William Olson for his help in getting TMI- and PR- retrieved rainfall data and also to Mr. Stephen Lang for proofreading the English in the paper. Acknowledgement is also made to NASA Goddard Space Flight Center for computer time used for this research.

References

Bauer, P., J.-F. Mahfouf, W. S. Olson, F. S. Marzano, S. D. Michele, A. Tassa and A. Mugnai, 2002: Error analysis of TMI rainfall estimates over ocean for variational data assimilation. *Q. J. R. Meteorol. Soc.*, **128**, 2129-2144.

Blackadar, A. K., 1976: Modelng the nocturnal boundary layer. *Preprints, Third Symp. on Atmospheric Turbulence, Diffusion, and Air Quality*, Raleigh, Amer. Meteor. Soc., 46-49.

———, 1979: High resolution models of the planetary boundary layer. *Advances in Environmental Science and Engineering*, Vol. 1, No. 1, J. Pfafflin and E. Ziegler, Eds., Gordon and Breach, 50-85.

Dudhia, J., 1993: A nonhydrostatic version of the Penn State-NCAR mesoscale model: Validation tests and simulation of an Atlantic cyclone and cold front. *Mon. Wea. Rev.*, **121**, 1493-1513

Grell, G. A., J. Dudhia, and D. R. Stauffer, 1995: A description of the fifth-generation Penn State/ NCAR mesoscale model (MM5). NCAR Technical Note, NCAR/TN-398 + STR, 138 pp. [Available from NCAR Publications Office, P. O. Box 3000, Boulder, CO 80307-3000].

Huffman, G. J., R. F. Adler, M. M. Morrissey, D. T. Bolvin, S. Curtis, R. Joyce, B. McGavock, J. Susskind, 2001: Global precipitation at one-degree daily resolution from multisatellite observations. *Journal of Hydrometeorology*, **2**, 36-50.

Huffman, G. J. and D. T. Bolvin, 2003: TRMM real-time multi-satellite precipitation analysis data set documentation. (Available at Code 912, NASA Goddard Space Flight Center, Greenbelt, MD 20771, USA)

Hou, A. Y., S. Q. Zhang, A. M. Da Silva, and W. S. Olson, 2000a:Improving assimilated global datasets using TMI rainfall and columnar moisture observations. *J. of Climate,* **13,** 4180-4195.

Kuo, Y.-H., and X. Zou, and Y. R. Guo, 1996: Variational assimilation of precipitable water using a nonhydrostatic mesoscale adjoint model. Part I: Moisture retrieval and sensitivity experiments. *Mon. Wea. Rev.*, **124**, 122-147.

Kummerow, C. , W. S. Olson, and L. Giglio, 1996: A simplified scheme for obtaining precipitation and vertical hydrometeor profile from passive microwave sensor. *IEEE Trans. Geosci. Remote Sens.,* **34,** 1213-1232.

Olson, W. S., C. D. Kummerow, G. M. Heymsfield, and L. Giglio, 1996: A method for combined passive-active microwave retrievals of cloud and precipitation profiles. *J. Appl. Meteor.*, **35**, 1763-1789.

Olson, W. S., C. D. Kummerow, Y. Hong, and W.-K. Tao, 1999: Atmospheric latent heating distributions in the Tropics derived from passive microwave radiometer measurements. *J. Appl. Meteor.,* **38**, 633-664.

Pu, Z.-X. and S. A. Braun 2001: Evaluation of bogus vortex techniques with four-dimensional variational data assimilation. *Mon. Wea. Rev.* , **129**, 2023-2039.

Pu, Z.-X., W.-K. Tao, S. Braun, J. Simpson, Y. Jia, J. Halverson, W. Olson, and A. Hou, 2002: The impact of TRMM data on mesoscale numerical simulation of Supertyphoon Paka. *Monthly Weather Review*. **130**, 2248-2258

Talagrand, O., 1997: Assimilation of pbservations, and introduction. *J. Meteorol. Soc. Japan*, **75**, 191-209

Zhang, D.-L., and R. A. Anthes, 1982: A high-resolution model of the planetary boundary layer — Sensitivity tests and comparisons with SESAME-79 data. *J. Appl.*

Meteor., **21**, 1594-1609.

Zou, X., W. Huang and Q. Xiao, 1998: A user's guide to the MM5 adjoint modeling system. NCAR TN-437+IA. MMM division, NCAR. [Available from NCAR Publications Office, P. O. Box 3000, Boulder, CO 80307-3000].

Zou, X. and Y.-H. Kuo, 1996: Rainfall assimilation through an optimal control of initial and boundary conditions in a limited-area mesoscale model. *Mon Wea. Rev.*, **124**, 2859-2882.

Zupanski, D. and F. Mesinger, 1995: Four-dimensional variational assimilation of precipitation data. *Mon. Wea. Rev.*, **123**, 1112-1127.

Table 1. Experimental Design

Experiment Number	Definition of W Term for rainfall	Physics Included	Bogus Vortex	Rainfall Assimilation
CTRL	No	Grell cumulus scheme Dudhia microphysics	No	No
1	Unified	Grell cumulus scheme Dudhia microphysics	No	Yes
2	20% error	Grell cumulus scheme Dudhia microphysics	No	Yes
3	Bauer	Grell cumulus scheme Dudhia microphysics	No	Yes
4	Bauer	Grell cumulus scheme	No	Yes
5	Bauer	Grell cumulus scheme Dudhia microphysics	No	Yes
6	Bauer	None	No	Yes
7	No	Grell cumulus scheme Dudhia microphysics	Yes	No
8	Bauer	Grell cumulus scheme Dudhia microphysics	Yes	Yes

Figure Caption

Fig.1 Rain rates (mm/hr) for two TMI swathes that passed over the Hurricane Bonnie (1998) around a) 1139 UTC 22 August 1998 and b) 1807 UTC 22 August 1998.

Fig.2 Variation of normalized cost-function with iteration number for Experiment 1 (dotted line), Experiment 2(dashed line) and Experiment 3(solid line).

Fig.3 Same as Fig.2, but for Experiment 4 (dotted line), Experiment 5 (solid line) and Experiment 6 (dashed line).

Fig.4 Hourly accumulated rainfall rate (mm/h) at the end of data assimilation (6h) for a) the control run (CTRL), b) Experiment 5 and c) the differences between a) and b).

Fig.5 Hourly accumulated rainfall rate (mm/h) at the end of data assimilation for assimilation of bogus wind only (Experiment 7).

Fig.6 Same as Fig.5, but both bogus wind and rainfall data assimilated (Experiment 8).

Fig.7 Histograms of probability density functions of 1-h rainfall amounts at the end of data assimilation for Experiment 7 (solid line with cross), Experiment 8 (solid line) and for TMI observations(solid line with dots).

Fig.8 Time series (3-h intervals) of a) maximum wind (m/s) at the lowest model level (about 50 m) and b) minimum sea-level pressure (hPa).

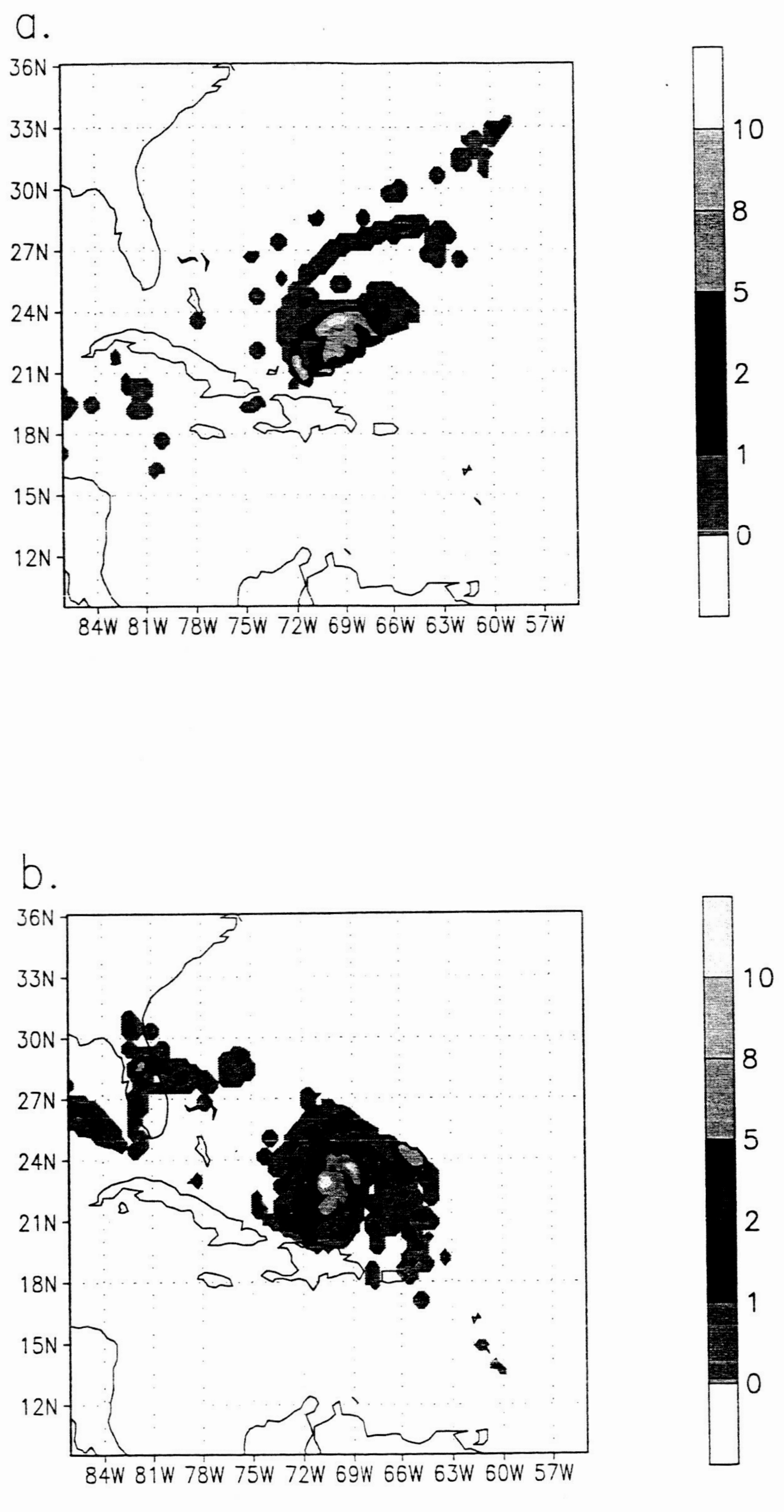
a.
36N
33N
30N
27N
24N
21N
18N
15N
12N
84W 81W 78W 75W 72W 69W 66W 63W 60W 57W
10
8
5
2
1
0
b.
36N
33N
30N
27N
24N
21N
18N
15N
12N
84W 81W 78W 75W 72W 69W 66W 63W 60W 57W
10
8
5
2
1
0

Fig. 1

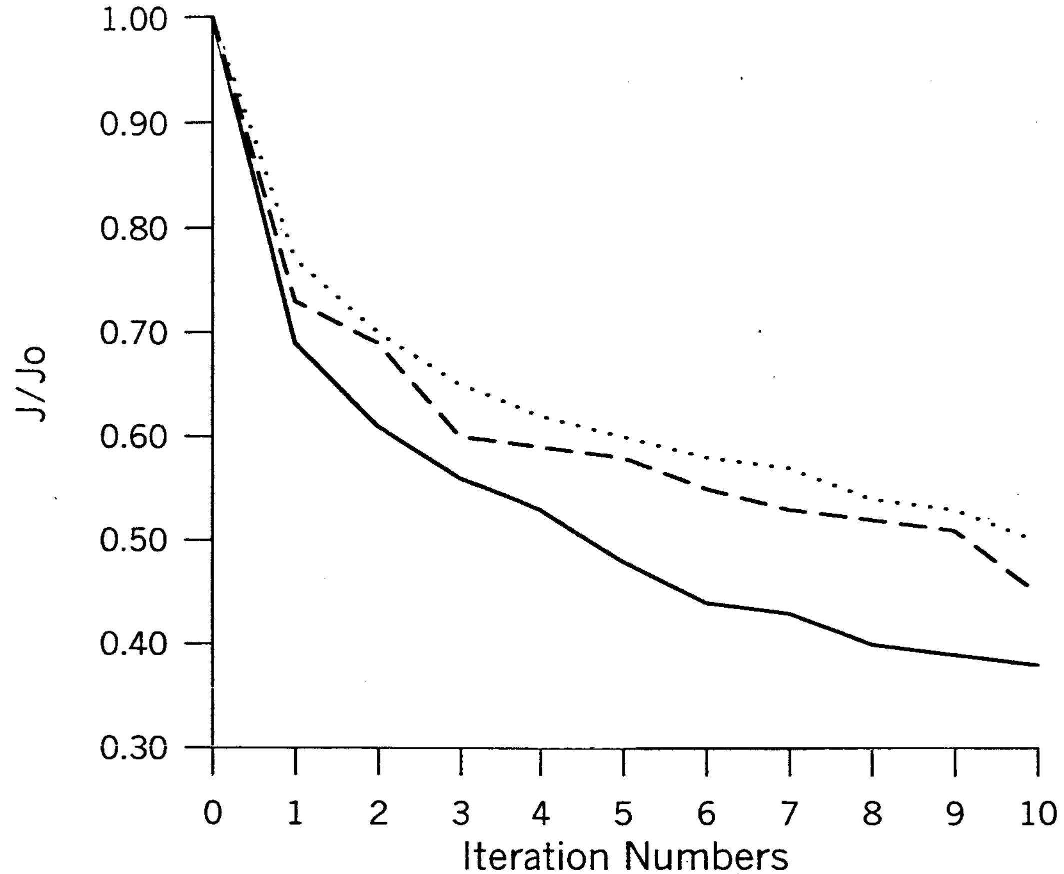
1.00
0.90
0.80
0.70
0.60
0.50
0.40
0.30
J/Jo
0
1
2
3
4
5
6
7
8
9
10
Iteration Numbers

Fig.2

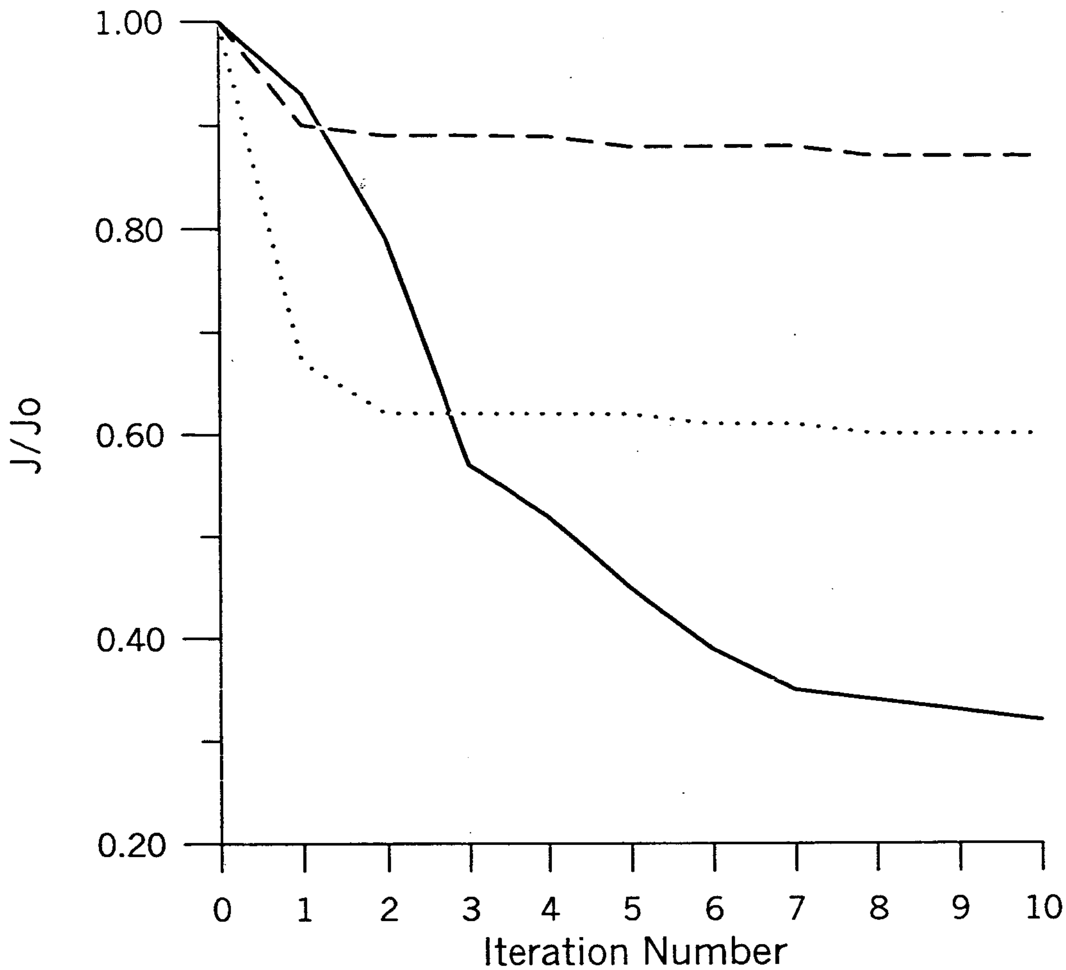

Fig.3

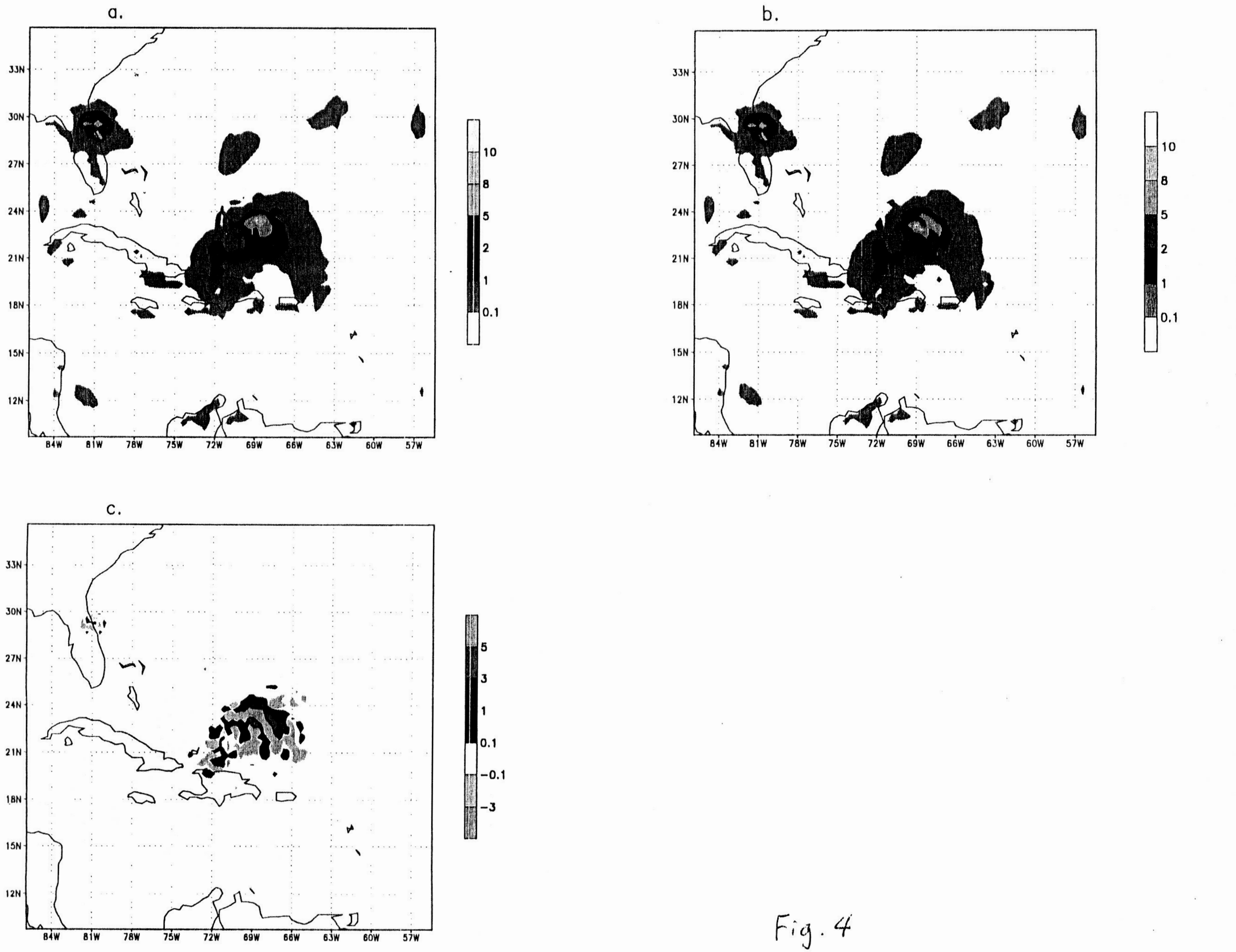
a.
b.
c.
33N
30N
27N
24N
21N
18N
15N
12N
84W
81W
78W
75W
72W
69W
66W
63W
60W
57W
0.1
1
2
5
8
10
5
3
1
0.1
-0.1
-3

Fig. 4

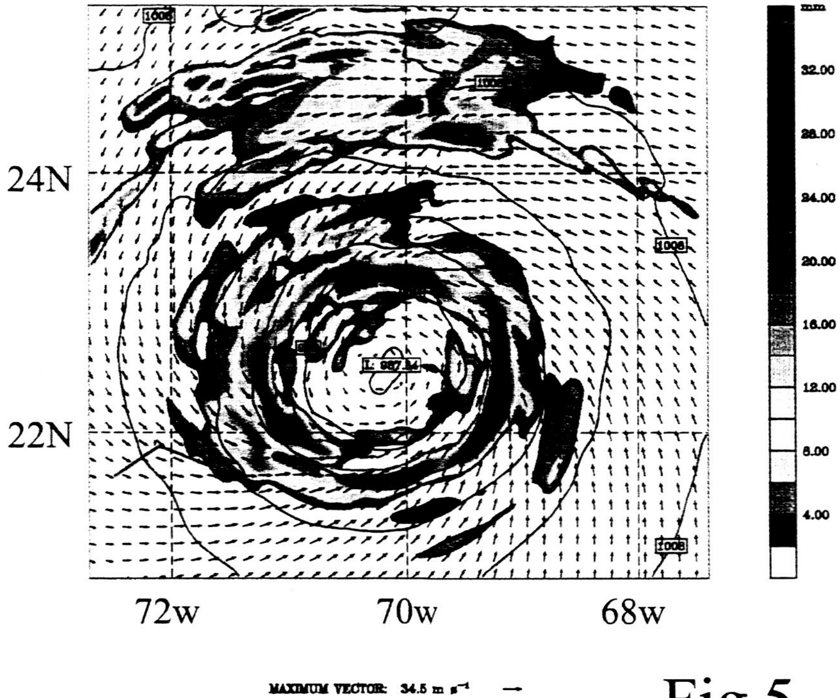
mm
32.00
28.00
24.00
20.00
16.00
12.00
8.00
4.00
24N
22N
72w
70w
68w
MAXIMUM VECTOR: 34.5 m s^{-1}

Fig.5

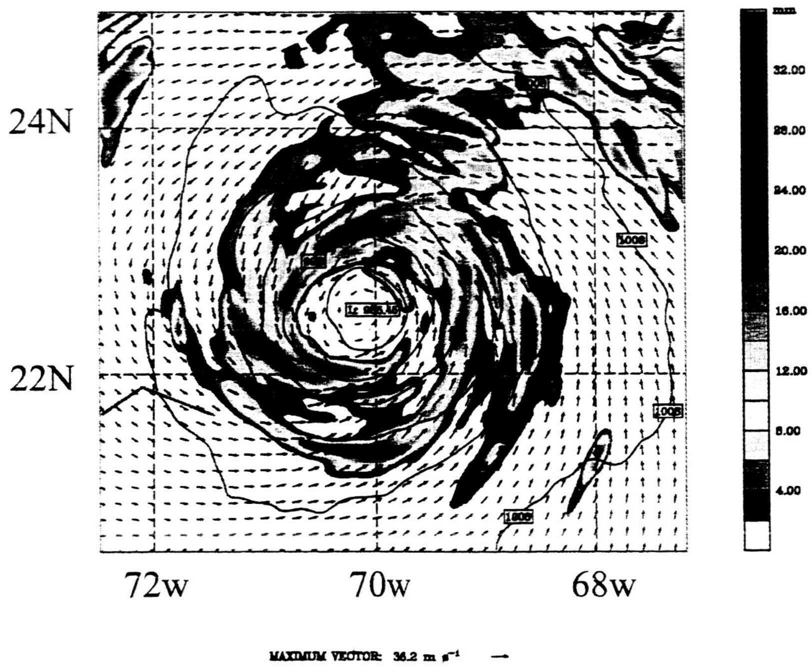
mm
32.00
28.00
24.00
20.00
16.00
12.00
8.00
4.00
24N
22N
72w
70w
68w
MAXIMUM VECTOR: 36.2 m s^{-1}

Fig.6

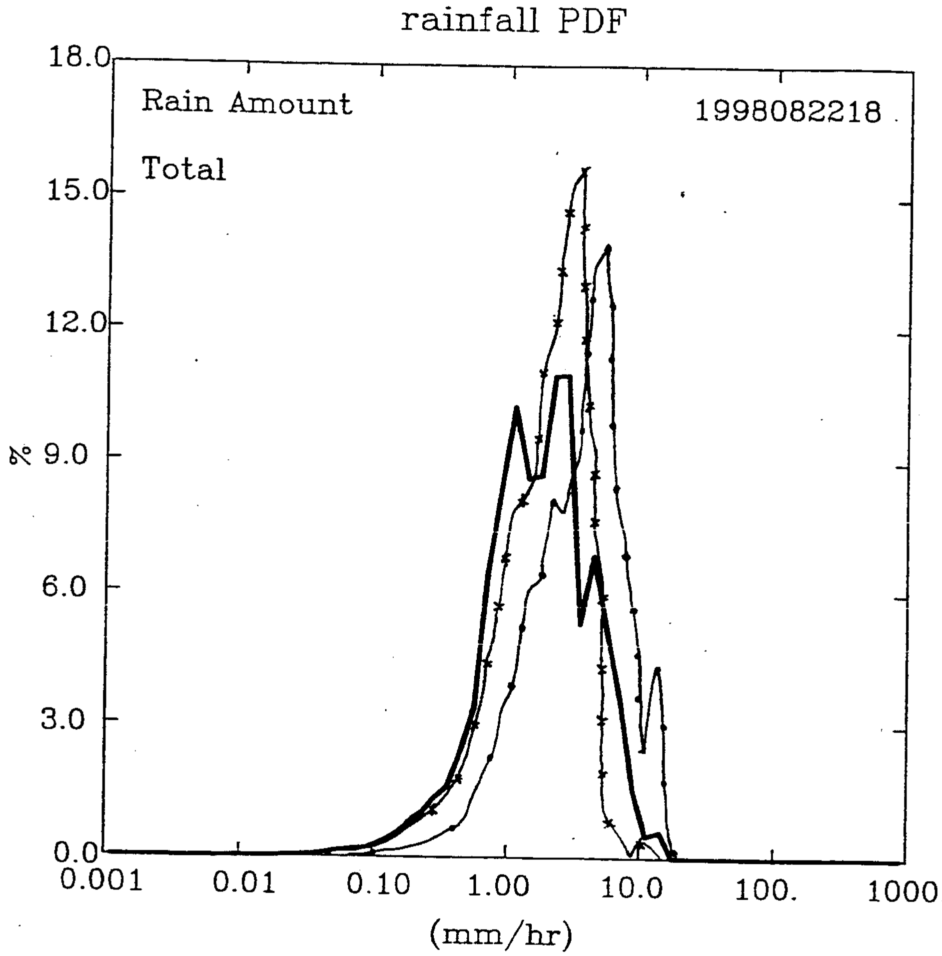
rainfall PDF
Rain Amount
Total
1998082218
18.0
15.0
12.0
9.0
%
6.0
3.0
0.0
0.001
0.01
0.10
1.00
10.0
100.
1000.
(mm/hr)

Fig. 7

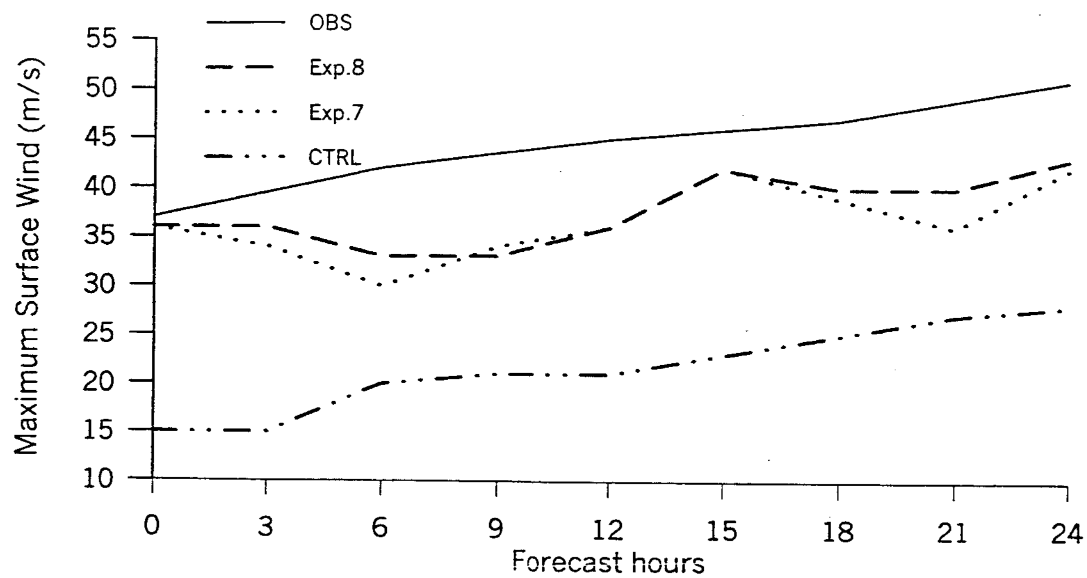

OBS
Exp.8
Exp.7
CTRL
Maximum Surface Wind (m/s)
55
50
45
40
35
30
25
20
15
10
0
3
6
9
12
15
18
21
24
Forecast hours

Fig.8 a

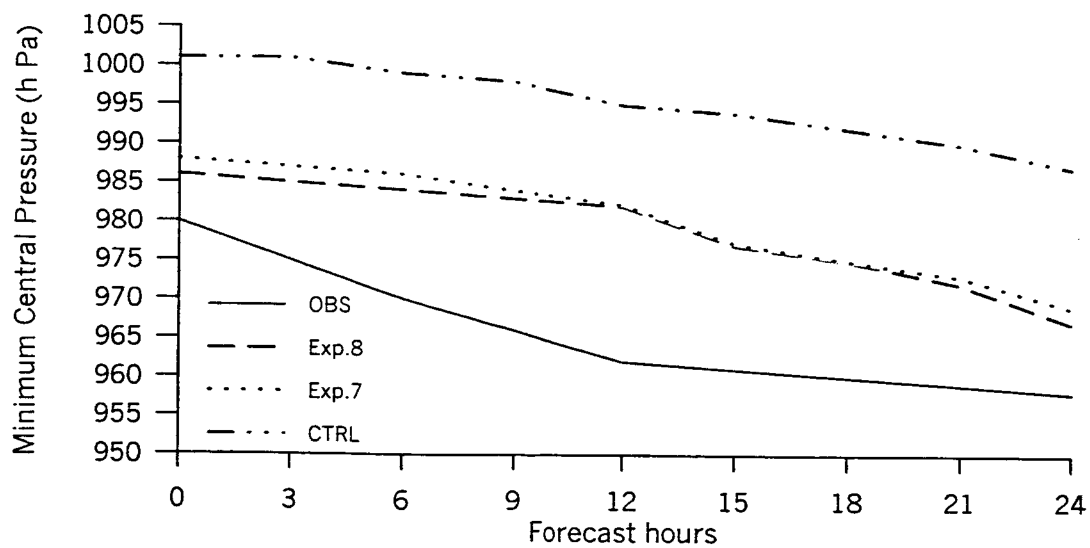

Minimum Central Pressure (h Pa)
1005
1000
995
990
985
980
975
970
965
960
955
950
OBS
Exp.8
Exp.7
CTRL
0
3
6
9
12
15
18
21
24
Forecast hours

Fig.8 b